

# Estimation of drying rate constant from static bed moisture profile by neural network inversion

M. K. Hazarika<sup>1\*</sup>, A. K. Datta<sup>2</sup>

(1. Tezpur University, Tezpur, Assam, India; 2. Indian Institute of Technology, Kharagpur, India)

**Abstract:** This study aims at extracting a mathematical expression for describing the moisture loss kinetics from grains dried in the form of a static bed, based on a measured grain moisture profile across the bed, and validating its reliability in predicting the drying times. The target expression for moisture transfer is the Lewis equation with Arrhenius type dependence of the drying rate constant on temperature, thereby reducing the problem to the determination of two coefficients (i.e.,  $E_a$  and  $K_0$ ) for the drying rate constant. The scheme of numerical solution of the non-equilibrium model of the deep bed drying process is represented as a trained neural network, with the values of the coefficients as inputs and the sum squared error (SSE) in the prediction of moisture content at various bed depths as the output. Training data for the neural network were generated for static bed drying of barley at an airflow rate of 638 kg/m<sup>2</sup>·h. The two coefficients were estimated by inversion of the trained neural network. The derived expression for drying rate constant was found to give a better prediction of the drying time and drying air temperature profiles at different experimental runs with air flow rates close to 638 kg/m<sup>2</sup>·h. It underlines the fact that grain moisture loss kinetics, extracted from a known moisture profile across the static bed can reliably be used to predict the batch drying time.

**Keywords:** static bed drying, non-equilibrium model, drying rate constant, bed moisture profile, neural network inversion, sum squared error

**Citation:** Hazarika, M. K., and A. K. Datta. 2014. Estimation of drying rate constant from static bed moisture profile by neural network inversion. *Agric Eng Int: CIGR Journal*, 16(1): 253–264.

## 1 Introduction

In case of deep bed drying processes, the estimation of the drying time for attaining a desired level of bed averaged moisture content, as well as the estimation of the distribution of moisture content in the grain bed, both, are of significant importance. A knowledge of the later would help preventing the over drying at the bottom layer and/or under drying at the upper layer. Over drying results not only in excessive energy consumption, but can even damage the quality of the dried material, especially in case of seeds. On the other hand, the grain will be vulnerable to mildew if the moisture content remains high.

As the in-situ methods for measuring moisture content are not straight-forward ones, development of suitable models is essential for this purpose and determination of time for completion of drying.

For describing the heat and mass transfer processes within the bed during static bed drying, several drying models have been developed which can be broadly divided into three categories, viz., logarithmic models, equilibrium models, non-equilibrium models or partial differential equation models. The non-equilibrium models consist of four partial differential equations and several relationships defining the initial and boundary conditions. They may be considered as exact theoretical models for grain drying when the appropriate assumptions are valid (Aregba et al, 2006).

In the non-equilibrium models the set of differential equations representing the states of the grain and drying

**Received date:** 2013-03-28 **Accepted date:** 2013-12-10.

\* **Corresponding author:** M. K. Hazarika, Department of Food Engineering and Technology, Tezpur University, P.O. Napaam, Tezpur -784028, India. Email: mkhazarika@tezu.ernet.in.

air in space and time, should be solved simultaneously. Solution of these models requires values of grain parameters, drying air parameters, and parameters representing the interaction of the drying air and the grain being dried, in the forms of heat and mass transfer coefficients. In one of such physical based models, first used by O'Callaghan et al. (1971) and later by other researchers (Farkas et al., 2000; Mandas and Habte, 2002), the moisture loss rate is written in the form of thin layer drying rate equation correlating the air flow rate, temperature and humidity with the moisture loss rate. More often, a relationship in the form of first order reaction kinetics is used and the rate constant, called the drying constant is expressed as a function of operating conditions. Even if an expression involving the effective diffusivity parameters is used (Ingram, 1976; Aregba et al., 2006), the rate equation remains an empirical one in nature due to inadequacy of information on the dependence of diffusivity on drying parameters.

It implies, within the limitations of the simplified assumptions and the accuracy of the mathematical methods used in solving the set of equations, when the non-equilibrium models are applied to simulate the drying process, the inadequacy of information on the dependence of moisture loss kinetics from grains on drying parameters may induce errors in the predicted drying behavior. To eliminate this possibility, it is proposed to characterize the drying behavior of the grains based on experimental deep bed drying data.

The present work aims at extracting a rule for representing the moisture loss kinetics from grains dried in the form of a static bed, from a measured grain moisture profile across the static bed, thereby eliminating the need for an already existing moisture loss equation derived based on thin layer drying experiments. The target expression for moisture transfer is the Lewis Equation with Arrhenius type dependence of the drying rate constant on temperature, thereby reducing the problem to the determination of two coefficients (i.e.,  $E_a$  and  $K_0$ ) for the drying rate constant. The extraction of drying rate parameters from drying behavior needs inverse mapping of the drying process. In an earlier work the authors proposed an algorithm for the derivation of an expression for the drying rate constant on the basis

of a correction rule, which uses the gradient of the cost function derived from the numerical solution of the physical model (Hazarika and Datta, 2004). In the present work a simplified approach is used, where for the forward mapping, the solution of the non-equilibrium model of the deep bed drying process is represented as a trained neural network, with the values of the unknown coefficients as the inputs and the sum squared prediction error (SSE) for moisture contents at various bed depths as the output. For the inverse mapping, the technique of neural network inversion is used, whereby the parameters of the drying rate constant are optimized to minimize the prediction error. Further, the deduced expression is used in the physical based deep bed drying model to predict the drying time for different experimental runs thereby to validate its usability in deep bed drying simulation. Considering the fact that not many reports are available on the use of inverse mapping ability of neural networks in drying simulation, an introduction on this topic is given in the next section.

## 2 Theoretical backgrounds

### 2.1 Neural networks

Neural networks are parallel machines, which model mathematical functions between inputs and outputs. They have the capacity to learn which allows them to gain knowledge through relationships in the training data. Instead of having to program them to perform in a certain way, one can just subject them to various data sets and let them induce the relationships between them. Although there are many different types of neural networks, many of the problems can most easily be represented by a feed forward neural network. A typical feed forward network consists of inputs, weights and an output as shown in Figure 1.

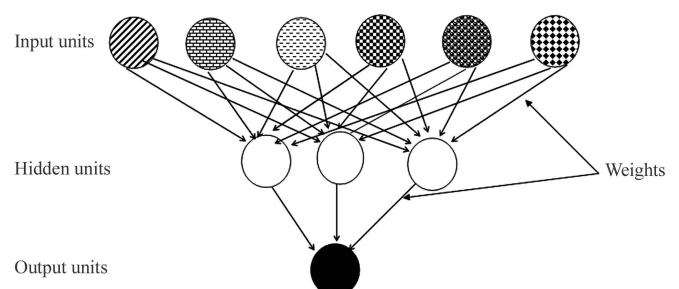


Figure 1 A feed forward neural network

The purpose of training a feed forward neural network is to determine a number of connection weights and their arrangement, called the architecture, and the magnitudes of the connection weights, which are derived on the basis of a set of training data. A trained feed forward neural network can be regarded as a nonlinear mapping from the input space to the output space. Once a feed forward neural network has been trained on a set of training data, all the weights are fixed. Thus, the mapping from the input space to the output space is determined. This mapping is referred to as the forward mapping. In general, the forward mapping is a many-to one mapping because each of the desired outputs usually corresponds to several different training inputs in the training set. Forward mapping is expressed mathematically as given in Equation (1).

$$\hat{y} = F(W, \hat{x}) \tag{1}$$

where,  $\hat{x}$  and  $\hat{y}$  represent the input and output of the network, respectively;  $W$  denotes the fixed weights, and  $F$  denotes the forward mapping determined by the architecture of the network. For a given input, it is easy to calculate the corresponding output from Equation (1).

### 2.2 Neural network inversion

In contrast to forward mapping as expressed by Equation (1), the problem of inverting a trained feed forward neural network is to find inputs which yield a given output. Such inputs are called the network inversions or simply inversions. The mapping from the output space to the input space is referred to as the inverse mapping (Equation (2)).

$$F^{-1} : \hat{y} = \hat{x} \tag{2}$$

The inverse problem is an ill-posed problem because the inverse mapping is usually a one-to-many mapping. In general, the inverse problem is locally ill-posed, in the sense that it has no unique solution and is globally ill-posed, because there are multiple solution branches (Lu et al. 1999). Hence, there is no closed form expression for the inverse mapping. In the past few years, several algorithms for inverting feed forward neural networks have been developed. A survey on this issue can be found in Jensen et al. (1999).

The first method of inverting feed forward neural

network were suggested separately by Kinderman and Linder in 1989 (Kinderman and Linder, 1990) and Williams in 1986 (Jensen et al., 1999). Both groups developed an iterative algorithm for inverting the feed forward network. In this algorithm, the inversion problem is set up as an unconstrained optimization problem and is solved by a gradient descent method, which is very similar to the back propagation algorithm. Another method to mention is from Lee and Kil in 1989 (Jensen et al., 1999).

However, Lu et al. (1999) have presented a straightforward method of inverting feed forward networks through the use of mathematical programming techniques. Their idea consists of formulating the inverse problem as a non-linear programming (NLP) problem, a separable problem or a linear programming problem depending on the structure of the neural network. One should note the advantage of employing this method as opposed to the others is that many times network inversions for multi-layer perceptions (MLP) can be obtained by solving the separable programming problem with the easier method used for linear programming problems. The non-linear programming approach to converge upon a solution for the inversion problem is used in this presented work.

As the aim of the present work is to use inverse mapping capability of neural network for estimation of drying rate parameter for the grains, it requires that the drying behavior of the static bed as a whole should be represented in the form of a neural network. The data to be used for training the neural network are: a set of varied combination of the coefficients  $E_a$  and  $K_0$  in drying rate constant as the inputs and the corresponding sum squared prediction error (SSE) in prediction of moisture contents, as obtained from static bed drying model solution, as the output. For the computation of the SSE in prediction of moisture contents, the non equilibrium model of static bed drying is solved numerically; the details of the model and the solution scheme are described in the next section.

### 2.3 Non-equilibrium deep bed drying model

The mass and energy balance in an elemental bed of unit cross section (Sharp, 1982) results in three differential equations:

Mass balance for moisture:

$$G \frac{\partial H}{\partial x} = -\rho_g \frac{\partial M}{\partial t} - \varepsilon \rho_a \frac{\partial H}{\partial t} \quad (3)$$

Energy balance of air:

$$G(c_a + c_v H) \frac{\partial T}{\partial x} = -\rho_g c_v (T - \theta) \frac{\partial M}{\partial t} - h(T - \theta) - \varepsilon \rho_a (c_a + c_v H) \frac{\partial T}{\partial t} \quad (4)$$

Energy balance for grain:

$$\rho_g (c_g + c_w M) \frac{\partial \theta}{\partial t} = h(T - \theta) + \lambda \frac{\partial M}{\partial t} \rho_g \quad (5)$$

Following Sharp (1982), if we consider the dryer consisting of a number of thin layers, and take into account the assumptions of previous workes (Mandas and Habte, 2002), the contribution of the time derivative terms  $\partial T / \partial t$  and  $\partial H / \partial t$ , in the above equations is very small for each thin layer, compared to the other terms in the system, and can thus be neglected. Rearranging, the system of PDEs can be reduced to following set of equations:

$$\frac{\partial H}{\partial x} = -\frac{\rho_g}{G} \frac{\partial M}{\partial t} \quad (6)$$

$$\frac{\partial T}{\partial x} = \frac{1}{G(c_a + c_v H)} \left( \rho_g c_v (T - \theta) \frac{\partial M}{\partial t} - h(T - \theta) \right) \quad (7)$$

$$\frac{\partial \theta}{\partial t} = -\frac{1}{\rho_g (c_g + c_w M)} \left( h(T - \theta) + \lambda \frac{\partial \theta}{\partial t} \rho_g \right) \quad (8)$$

The set of Equation 6 to Equation 8 involves four unknowns viz.,  $M(x, t)$ ,  $\theta(x, t)$ ,  $H(x, t)$  and  $T(x, t)$ . The fourth equation used along with Equation (6) to Equation (8) to solve for these unknowns is the drying rate equation. For barley, Lewis equation is used (Sharp, 1982; Sun and Woods, 1997), which is written as below.

$$\frac{\partial M}{\partial t} = -k_d (M - M_e) \quad (9)$$

where,  $k_d = K_0 \exp(-E_a / T)$

here,  $E_a$  and  $K_0$  are the two coefficients, having specific values for material being dried.

### 2.4 Scheme of numerical solution

For the numerical solution of the set of Equation (6) to Equation (9), the scheme of solution suggested by Mandas and Habte (2002) is used. The discretization scheme is shown in Figure 2.

The method suggested by Mandas and Habte (2002)

adopts an iterative predictor–corrector process for solving the two expressions, i.e., Equation (8) and Equation (9), in the time domain, and a first-order scheme that resorts to an iterative process for the other two expressions, i.e., Equation (6) and Equation (7), in the space domain.

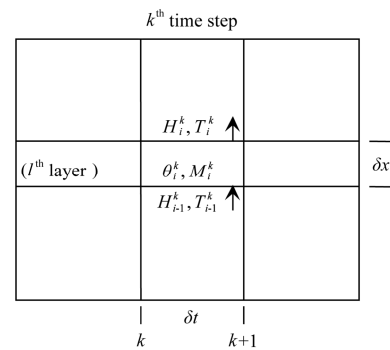


Figure 2 Schematic representation of the  $i^{th}$  thin layer of depth increment  $\delta x$  in a static-bed drier at the time step  $k$

Based on the values of  $H$ ,  $T$ ,  $M$ , and  $\theta$  at a given time step  $k$ , for  $i^{th}$  layer, the values of  $M$  and  $\theta$ , for the time step  $k+1$  are calculated in an iterative manner, using the Equations (11) and Equation (12)

$$M_i^{k+1} = M_i^k + \delta t \cdot \left( \frac{\partial M}{\partial t} \right)_{ave}^k \quad (11)$$

$$\theta_i^{k+1} = \theta_i^k + \delta t \cdot \left( \frac{\partial \theta}{\partial t} \right)_{ave}^k \quad (12)$$

At the end of the predictor–corrector step, one will have the moisture content and grain temperature for layer  $i$  at time  $k+1$ . For the same layer, the exit air temperature and humidity are calculated using the finite-difference procedure (Equation (13) and Equation (14)):

$$H_{i+1}^{k+1} = H_i^{k+1} + \delta x \cdot \left( \frac{\partial H}{\partial x} \right)_i^{k+1} \quad (13)$$

$$T_{i+1}^{k+1} = T_{i0}^{k+1} + \delta x \cdot \left( \frac{\partial T}{\partial x} \right)_i^{k+1} \quad (14)$$

### 3 Materials and method

The various steps involved in the scheme to deduce an expression of drying rate constant ( $k_d$ ) in the form of the Equation (10) for barley based on deep bed drying experimentation are: selection of physical property parameters, selection of a range of values for simulation, numerical solution of the set of differential equations,

generation of training data for the neural network, training of neural network to represent the solution of the numerical scheme, inversion of the trained network and derivation of an expression for drying rate constant, and validation by comparison with existing expressions and simulation of static bed drying process with the derived expression.

**3.1 Physical property parameters**

**3.1.1 Coefficients and properties for barley**

For few properties of barley, relationships are available from literatures. O’Callaghan et al. (1971) used the following relation for volumetric heat transfer coefficient for barley.

$$h = h(G, p, T) = 856800 \left[ \frac{G(T + 273)}{P_{atm}} \right] \tag{15}$$

For equilibrium moisture content many expressions are available, and Sun and Wood (1997) listed four such expressions. In the original model of O’Callaghan (1971), the Boyce Equation (Boyce, 1965) was used which has quite a different form than other models. The model of Bowden et al. (1983) is used in this study (Equation (16)).

$$M_e = M_e(T, RH) = 0.143 - 0.016 \ln(T) - 0.079 \ln(1 - RH) \tag{16}$$

Within the restrictions suggested in Mandas and Habte, (2002), the value of heat of desorption of water has been assumed to be equal to that of latent heat of vaporization.

**3.1.2 Other property data**

The property data, as was used by O’Callaghan et al. (1971), and later used by Farkas et al. (2000), and Mandas and Habte (2002); are used in this work and are given in Table 1.

**Table 1 Physical property values used in the study**

Density of barley ( $\rho_g$ )	600 kg m <sup>-3</sup>
Heat of water desorption ( $h_o$ ) at 0°C	2501700 J kg <sup>-1</sup>
Specific heat of dry barley ( $c_g$ )	1300 J kg <sup>-1</sup> K <sup>-1</sup>
Specific heat of dry air ( $c_a$ )	1005 J kg <sup>-1</sup> K <sup>-1</sup>
Specific heat of water vapour ( $C_v$ )	1820 J kg <sup>-1</sup> K <sup>-1</sup>
Specific heat of water ( $C_w$ )	4187 J kg <sup>-1</sup> K <sup>-1</sup>

**3.2 Range of values for simulation**

For the drying rate constant of barley, different relations are available in the literature. Out of the total

five expressions for drying rate constants, as listed by Sun and Woods (1997), four have Arrhenius type temperature dependence. These models are listed in the Table 2.

To include the values used in these expressions listed in Table 2, the ranges of values for simulation were selected within the range of values 1.0 to 350000 for  $K_0$  and 3000 to 7000 for  $E_a$ .

**Table 2 Various models for drying rate constant (Equation (10)) of barley (Sun and Woods, 1997)**

Model name	$K_0$ (s <sup>-1</sup> )	$E_a$ (K)
Sun and Woods	1.416	3258
Boyce	3.900	3086
Bruce	139.300	4426
Jayas and Sukhansanj	348500.000	6942

**3.3 Numerical solution**

The numerical solution was carried out by implementing the scheme described in section 2.4 as a MATLAB code. The first question to be addressed was about the number of layers i.e., space discretization. For the experimental run B126 (experimental conditions are specified in Ttable 3), end of drying moisture content measurements are available at 12 equally spaced locations across the depth. First of all it is assumed that these moisture values are representative of the moisture content of 12 layers of the bed. Each of these 12 layers were divided in such a way that the middle layer correspond to the cells at which the moisture contents were known. For this purpose, an expression (Equation (17)) similar to one suggested by Farkas et al. (2000) was used to determine the most appropriate thickness of the grain.

$$N_k = 12 \times 3^k \tag{17}$$

where,  $k = 1, 2, \dots, k$ .

Simulation trials with increasing number of layers were performed until the differences in temperature and moisture content of the middle layer between the last two trials were less than 1°C and 1% d.b., respectively. As the difference between 12 and 36 layers were found to be sufficiently small, 36 layers were used for the simulation. A time step of 1.0 s was selected for the simulation.

**3.4 Development of neural network model**

The motivation of the present work is to substitute the

model solution for Equation (6) to Equation (9) with a neural network model, so that through the inversion of the trained neural network, a desired input condition can be determined to achieve a targeted outcome. Here, the targeted outcome chosen is minimum value of sum squared error (Equation (18)) of model predicted end-of-drying moisture profile in comparison with an experimentally observed profile. Further, this approach is applied here for model parameter update, i.e, updating the model parameter of the drying rate constant for static bed drying of barley under specified conditions. Accordingly, the proposed neural network model will have drying rate constant model parameters as the input and SSE, as defined by Equation (18), as the output for a given drying condition. On inversion of the neural network for a minimum possible SSE, a set of parameter for drying rate constant can obtained to update the moisture loss rate equation (Equation (9)) and to use in combination with Equation 6 to Equation (8) as the static bed drying model equation.

$$SSE = \frac{1}{2} \sum_{i=1}^{12} \left\{ \frac{(m_i)_{exp} - (m_i)_{sim}}{(m_i)_{exp}} \right\}^2 \quad (18)$$

#### 3.4.1 Data for ANN model development

Table 3 lists a set of experiments conducted previously in on static bed drying of barley (O' Callaghan, 1971; Boyce, 1965). The drying condition were specified by grain bed depth (30 cm), inlet air temperature as indicated in Table 3, air flow rate as indicated in Table 3, inlet air humidity 0.006 kg vapour/kg dry air, and initial grain temperature of 21°C. The common measurement in all the experimental runs were bed averaged moisture content at the end of specified drying time. These data are useful in validating the static bed drying model, whether the model predicts correct drying time to achieve desired final bed average moisture content.

Further, experimental run B126 with the experimental conditions specified in Table 3 has been reported with an end of drying measured moisture profile with 12 moisture content measurements at 12 equally spaced locations (O' Callaghan, 1971; Boyce, 1965). These data have been used by Callaghan (1971) and by Mandas and Habte

(2002) for comparing their results. In the present work, this moisture profile will be used for static bed drying model parameter updating by neural network inversion method.

**Table 3 Experimental drying times for validation of extracted drying rate constant**

O' Callaghan's test Run No	Inlet air temp /°C	Air flow rate /kg (m <sup>2</sup> ·h) <sup>-1</sup>	Initial mc (db) /kg kg <sup>-1</sup>	Final mc (db) /kg kg <sup>-1</sup>	Drying time /min
B 126	68	638	0.352	0.225	160
B 134	68	640	0.342	0.14	255
B 139	60	303	0.346	0.289	157
B 137	60	312	0.34	0.14	568
B 138	60	314	0.34	0.194	447
B 141	60	315	0.344	0.229	327
B 142	60	311	0.34	0.257	215
B 122	68	310	0.337	0.298	105
B 147	68	320	0.345	0.133	521
B 118	68	312	0.332	0.177	390
B 120	68	311	0.35	0.224	303
B 121	68	315	0.353	0.268	200
B 145	68	638	0.343	0.302	57
B 146	68	643	0.345	0.182	211
B 125	68	635	0.346	0.262	105

Similarly, for experimental run B134 with the experimental conditions specified in Table 3, drying air temperatures at various depths have been reported in works of O' Callaghan, (1971), and Boyce (1965). These temperature profiles will be used for validating the static bed drying model with updated parameters.

At experimental conditions of B126 experimental run, numerical computation of the deep drying model was carried out with combination of values of  $K_0$  and  $E_a$  within the range of 1.0 to 350000 for  $K_0$  and 3000 to 7000 for  $E_a$  to predict the end of drying period moisture profile at locations corresponding to the measurement locations. Out of the 36 layers as specified in section 3.3, these locations correspond to  $(2+3i)^{th}$  layer of the drying bed. The SSE for moisture values at all these layers was calculated using the Equation (18) from numerically computed values of the cell moisture and available measurement values. Representative values of the inputs and outputs for the proposed neural network are given in Table 4.

**Table 4 A part table of input and output of the neural network model**

Inputs		output	Inputs		output
$K_0$	$E_a$	SSE	$K_0$	$E_a$	SSE
3500	7000	0.128321	350	7000	0.140691
3500	6500	0.095144	350	6500	0.135823
3500	6000	0.035218	350	6000	0.117622
3500	5500	0.001703	350	5500	0.069300
3500	5000	0.014492	350	5000	0.012164
3500	4500	0.031636	350	4500	0.004807
3500	4000	0.171416	350	4000	0.026678

**3.4.2 Neural network model development**

For the purpose of neural network training, data were normalized by using MATLAB routines. The developed ANN model has two output nodes, representing  $K_0$  and  $E_a$  and one output node representing the prediction SSE. Created MLP was trained by the scaled conjugated gradient algorithm using the codes from the toolbox NETLAB as available online at <http://www.ncrg.aston.ac.uk/netlab>.

**3.5 Inversion of trained neural network**

Inversion was carried out by the method of non linear optimization, of Lu et al. (1999). The method is summarized in Equation (19).

$$\text{Minimize } p(\hat{x}) \tag{19}$$

Subject to  $F(W, \hat{x}) - \hat{y} = 0$   
 $a < x_i < b$

Here  $F(W, \hat{x})$  is the representation of the forward mapping of the feed forward network,  $\hat{x}$  refers to the inputs and  $W$  to the weights.  $\hat{y}$  is the given output of the inversion problem and  $a$  and  $b$  refer to the range the inputs must fall between.  $p(\hat{x})$  is called the objective function and it is the function which must be minimized.

Here,  $\hat{x}$  refers to the vector which satisfies all the constraints that are stated and provides a solution to the NLP problem. The purpose of  $p(\hat{x})$  is to express what kind of inversions are to be computed. In this study,  $p(\hat{x})$  is set such that the inputs which satisfy the inversion and those which are the lowest of all the possible solutions are picked during the inversion. Inversion of the network yields normalized values of the  $E_a$  and  $K_0$ .

**3.6 Validation of extracted parameters**

Normalized values of the  $E_a$  and  $K_0$  obtained by neural network inversion was de-normalized to get extracted parameters  $E_a$  and  $K_0$  for drying constant. The derived expression for drying constant was compared with existing models listed in Table 2 for temperature dependence. The derived expression for drying constant was used in static bed drying model Equation (6) to Equation (9) to estimate the drying time for experimental runs B126, B134, B139, B137, B138, B141, B142, B122, B147, B118, B120, B121, B145, B146 and B125 with conditions given in Table 3. Improvement in the prediction of drying time with respect to earlier work of O’ Callaghan (1971) and Mandas and Habte (2002) for these runs would indicate that the drying rate constant expression derived from end of drying moisture profile updates the static bed drying model parameter for better prediction. Further the model was used to predict the air temperature profile across the bed over the whole drying period, for the test run B134, to present a qualitative validation of the predictability of the updated model.

**3.7 Assumptions and limitations of the model**

The neural network model was developed for a fixed drying condition in terms of air velocity, drying temperature and air humidity. In this case, the moisture profile obtained from experimental run B126 with experimental conditions specified in Table 3 was only used to estimate the parameters of the drying rate constant. Due to the form of Equation (10), the effects of air temperature get modeled. However, the expression does not have a term to model the effects of air flow rate. Therefore, the model obtained by combining Equation (6) to Equation (9), with updated parameters of Equation (10) will have validity within the range of operating conditions used in developing the neural network model.

**4 Results and discussion**

The error surface of the objective function, defined by Equation (18), for the selected values of  $E_a$  and  $K_0$  is shown in the Figure 3, which shows a valley of the minimum values of the SSE. This indicates the possibility of having more than a single combination of

the coefficients along this valley leading to a SSE values in the close vicinity of the minimum SSE within the selected range values of coefficients, i.e., more than one combination of input parameters for the minimum SSE. This can be eliminated by putting constraints during the inversion of the neural network.

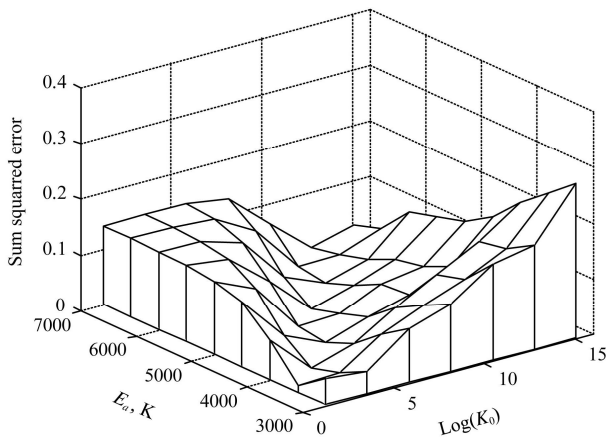


Figure 3 The error surface of the SSE values in the prediction of the moisture content at 12 points across the depth of the static bed

The data points were used to train a feed forward neural network, trained with the scaled conjugated gradient algorithm. The architecture of 2-10-1 was found to be giving an error of less than  $10^{-4}$ , and, beyond it the raising of the number of hidden neurons did not yield further lowering of the error. The trained network with the architecture of 2-10-1 is selected as the mapping of the SSE in prediction of moisture profile with respect to the coefficients of the drying rate constant. The plot of the training data and the NN predicted data is shown in Figure 4.

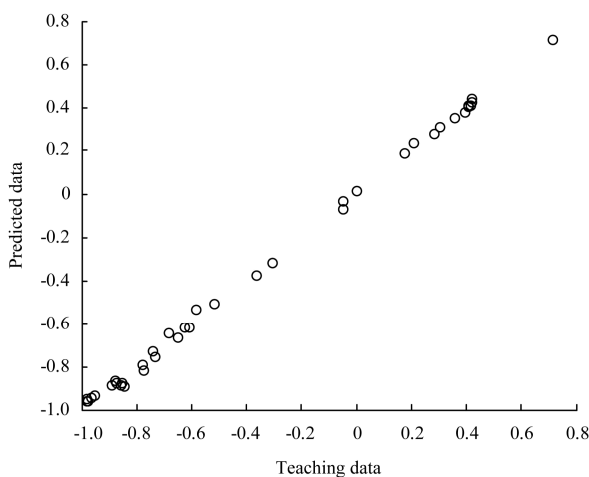


Figure 4 Plot between the teaching data and predicted data by the trained neural network

The inversion of the network was carried out for a minimum possible value (preferably zero) of the SSE defined in Equation (18). The approach of systematic lowering of the desired SSE value was followed, through which the trained net could be inverted for a SSE of 0.00275. Corresponding values of the  $E_a$  and  $K_0$  obtained were calculated to be 5,720 K and 7,943.3  $\text{s}^{-1}$  respectively. Due to the lack of convergence of the search further reduction in SSE was not possible. Accordingly, the extracted expression for drying rate constant is (Equation (20))

$$k_d = 7943.3 \exp(-5720 / T) \quad (20)$$

This expression, which was derived on the basis of a single moisture profile of static bed drying at an air flow rate of 638  $\text{kg} (\text{m}^2 \cdot \text{h})^{-1}$  was compared with the existing equations listed in Table 2, by plotting the variation of the value of the drying rate constant with temperature as shown in Figure 5.

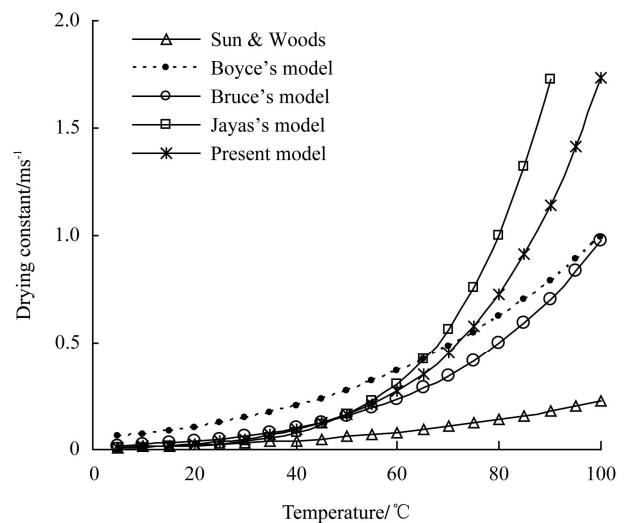


Figure 5 Comparison of the temperature dependence of the derived model with few existing Arrhenius type models of drying rate constant

From Figure 5 it can be observed that out of the four existing equations, which probably were derived from moisture loss history of thin layers of the grains, the derived expression closely follows the expression given by Jayas and Sukhansanj (ref. from Sun and Woods, 1997), and that of Bruce (ref. from Sun and Woods, 1997), up to the temperature of around 55 $^{\circ}\text{C}$ . Beyond this temperature it lies between these two models, being little less sensitive to rise in temperature than that by the



model of Jayas and Sukhansanj. Accordingly the performance of the derived expression will be closely observed in comparison to the predictive ability of the model of Jayas and Sukhansanj (ref. from Sun and Woods, 1997). As the drying air temperature in the experimental run was 68°C only, the obtained expression should be considered to be reliable up to this temperature only.

The predicted moisture distribution across the depth of the grain bed is presented in Figure 6, along with the predictions by Mandas and Habte (2002), which used the Bruce’s model; and the prediction using the equation of Jayas and Sukhansanj in the model, for the same final moisture content. The predicted profile obtained by using this extracted equation, as well as the one obtained by using the equation of Jayas and Sukhansanj, are closely following the experimental pattern, while there is considerable deviation for the moisture profile obtained by the use of Bruce’s model.

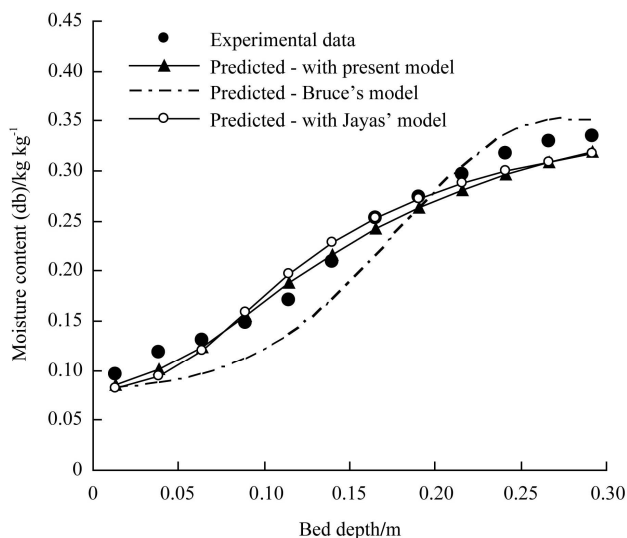


Figure 6 Comparison of the predicted moisture profile with experimental data, the prediction being based on the drying rate constant derived from the moisture profile

The performance of the extracted equation in predicting the drying time for all the 15 experimental runs is compared with that obtained by using the equation of Jayas and Sukhansanj (ref. from Sun and Woods, 1997), and results of Mandas and Habte (2002). The comparison of the predicted and the experimental drying times is shown in Table 5 with the expression of percent

error in prediction in drying time given by Equation (21).

Percent Prediction Error of drying time = 100

$$\times \frac{(drying\ time)_{exp} - (drying\ time)_{sim}}{(drying\ time)_{exp}} \quad (21)$$

It can be seen that the drying time predicted by this updated model is better than the estimated values reported by Mandas and Habte (2002). In all runs Mandas and Habte’s computation (Mandas and Habte, 2002), estimated a lower drying time yielding a negative percent error of prediction. The updated model resulted in the lowest SSE of the percentage error in the prediction of drying time, a value of 680 in the present study, whereas corresponding values for the works of Mandas and Habte (2002) was 1640. When the model of Jayas and Sukhansanj (ref. from Sun and Woods, 1997) was used the predicted drying time was obtained almost same as that obtained with the extracted model, and the SSE was 716. It indicates that the performance of the extracted equation is comparable with that of the equation of Jayas and Sukhansanj (ref. from Sun and Woods, 1997).

Experimental runs B126, B134, B145, B146 and B125 were carried out with the air flow rate of 635-643 kg/(m<sup>2</sup>·h), which is close to the flow rate at which the moisture distribution pattern is available for extracting the drying rate constant i.e., 638 kg/(m<sup>2</sup>·h). In three out of these five of the experimental runs the predicted drying time is almost same, the mean square of percent error (MSE) 13.6. However, experimental runs B139, B137, B138, B141, B142, B122, B147, B118, B120, and B121 were carried out at a lower air flow rates, in the range of 303-320 kg (m<sup>2</sup>·h)<sup>-1</sup>. Therefore, the updated drying constant model may not be considered to be valid for this range. For comparison purpose, the MSE for these 10 experiments was found to be 134.6 the predicted drying times appeared to be higher than the experimentally observed value. This indicates a limitation in the validity of the updated model. However, a similar trend was observed when the equation of Jayas and Sukhansanj (ref. from Sun and Woods, 1997) was used in the static bed drying model. Both these models have the similar general limitation of failing to take account of effect of air flow rates.

**Table 5 Comparison between the experimental and predicted drying times for present study with the work of Mandas and Habte (2002)**

Test Run No	Drying time /min	Predicted drying time/min			Percent prediction error		
		Result of Mandas & Habte (2002)	Computed with $k_d$ of Jayas & Sukhansanj	Computed with derived $k_d$	Result of Mandas & Habte (2002)	Computed with $k_d$ of Jayas & Sukhansanj	Computed with derived $k_d$
B 126	160	144	162.9	161	-10	2	1
B 134	255	261	275.3	272	2	8	7
B 139	157	139	180.3	180	-11	15	15
B 137	568	518	610.6	605	-9	7.5	7
B 138	447	349	435	435	-22	-3	-3
B 141	327	265	342	342	-19	4.5	5
B 142	215	192	253	253	-11	18	18
B 122	105	79	130	130	-25	24	24
B 147	521	457	533	530	-12	2.5	2
B 118	390	328	398	398	-16	2	2
B 120	303	252	323	324	-17	6.5	7
B 121	200	165	218	218	-18	9	9
B 145	57	48	56.95	56.7	-16	0	-1
B 146	211	194	211.9	209	-8	0.5	-1
B 125	105	95	109.75	109	-10	4.5	4
Values of the sum squared error				1640	716	680	

For validating the reliability of the extracted equation to use in deep bed simulation of barley one more criteria, viz. comparison of the air temperature profiles at different depths of the bed was used. The drying condition was: a static bed 0.305 m deep, initially at a moisture content of 0.342 as dried with air at 68°C, and humidity of 0.006 kg (kg dry air)<sup>-1</sup> and at a flow rate of 638 kg (m<sup>2</sup>·h)<sup>-1</sup> (Run no B134 in Table 3). Air temperatures were determined at points in the bed 0.025 m, 0.076 m, 0.152 m, 0.229 m and 0.305 m from the air inlet. The comparison of the predicted and measured temperature profiles is shown in Figure 7. From the plot (Figure 7) it can be seen that except at the bottom layers, the predicted temperature profiles matches the observed temperature profile after a lag only, increasing lag for the upper layers. To verify, if this behavior is specific to the derived expression only, temperature profiles at the same bed depths were obtained using the equation of Jayas and Sukhansanj (ref. from Sun and Woods, 1997) as well. Both the calculated profiles found to be almost overlapping with each other. The existence of such a lag between the predicted and the observed temperature profile was found even when the

diffusion based model was used in the simulation (Ingram 1976), hence may be considered as a general limitation of deep bed drying models.

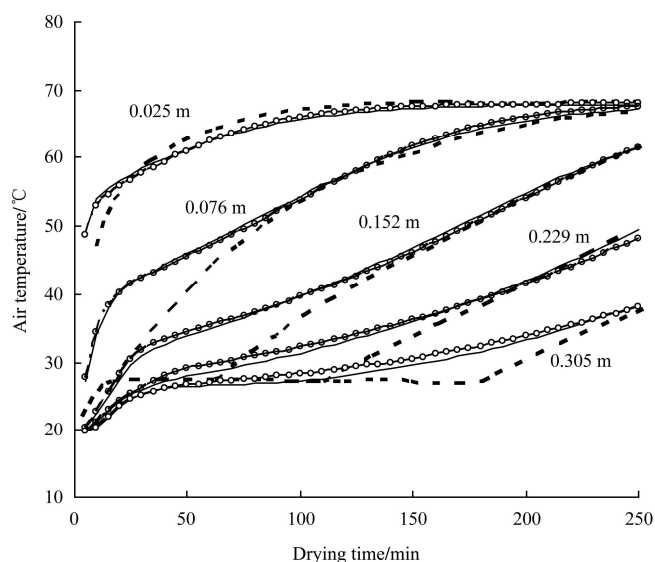


Figure 7 Comparison of the predicted air temperature profiles with experimental data (---), with one prediction being based on the drying rate constant derived in the present work (—) and the other being based on equation of Jayas and Sukhansanj (-o-o-o-)

As the concern in the present study has been the verification of the reliability of the extracted equation in

mapping the drying behavior of the grain, and thermodynamics of the drying air, it can clearly be observed that its performance matches that of the equation by Jayas and Sukhansanj (ref. from Sun and Woods, 1997), with marginal improvements in the predicted values.

### 5 Conclusions

1) Neural network inversion, as a tool, could extract an expression for drying rate constant based on bed moisture profile during static bed drying.

2) Neural network inversion based on end of drying bed moisture profile of barley extracts an expression for drying rate constant customized to incorporate temperature dependence.

3) Based on the derived drying rate expression, the prediction error in drying time was found to be lower than works reported by earlier workers.

Hence, the technique of neural network inversion using bed moisture profile can reliably be used to extract rule for moisture loss kinetics in static bed drying, for simulating the kinetics of static bed drying in subsequent runs.

### Nomenclature

$c_a$  specific heat of dry air,  $J\ kg^{-1}\ K^{-1}$   
 $c_g$  specific heat of dried solid,  $J\ kg^{-1}\ K^{-1}$   
 $c_v$  specific heat of water vapour,  $J\ kg^{-1}\ K^{-1}$   
 $c_w$  specific heat of water,  $J\ kg^{-1}\ K^{-1}$

$E_a$  coefficient (exponent) in the expression for drying rate constant, K  
 $G$  specific mass flow rate of air,  $kg\ m^{-2}\ s^{-1}$   
 $H$  absolute humidity of air,  $kg\ [kg\ (dry\ air)]^{-1}$   
 $h$  grain bed volumetric heat transfer coefficient,  $J\ m^{-3}\ K^{-1}\ s^{-1}$   
 $i$  index for a layer in the bed.  
 $K_d$  drying rate constant,  $s^{-1}$   
 $K_0$  coefficient in the expression for drying rate constant,  $s^{-1}$   
 $M$  moisture content of grain, in decimal dry basis,  $kg\ [kg\ (dry\ matter)]^{-1}$   
 $M_e$  equilibrium moisture content of grain, in decimal dry basis,  $kg\ [kg\ (dry\ matter)]^{-1}$   
 $p(\hat{x})$  cost function for optimization  
 $RH$  relative humidity of air  
 $T$  air temperature, K  
 $\theta$  grain temperature, K  
 $\lambda$  heat of water desorption, J/kg  
 $W$  weight matrix of the neural network  
 $\hat{x}$  input vector for a neural network  
 $\hat{y}$  output vector of a neural network  
 $\hat{y}l$  desired output vector for inversion of the neural network  
 $\delta x$  depth increment, m  
 $\varepsilon$  void ratio  
 $\rho_a$  density of air,  $kg\ m^{-3}$   
 $\rho_g$  density of grain,  $kg\ m^{-3}$

### References

Aregba, A. W., P. Sebastian, and J. P. Nadeau. 2006. Stationary deep-bed drying: A comparative study between a logarithmic model and a non-equilibrium model. *Journal of Food Engineering*, 77 (1): 27-40.

Bowden, P. J., W. J. Almond, and F. A. Smith. 1983. Simulation of near ambient grain drying. I. Comparison of simulation with experimental results. *Journal of Agricultural Engineering Research*, 28 (4): 279-300.

Boyce, D. S. 1965. Moisture and temperature changes with position and time during drying. *Journal of Agricultural Engineering Research*, 10 (4): 333-341.

Farkas, I., P. Remenyi, and A. Biro. 2000. Modelling aspects of grain drying with a neural network. *Computers & Electronics in Agriculture*, 29 (1-2): 99-113.

Hazarika, M. K., and A. K. Datta. 2004. Dynamic neural network based simulation of static bed drying of barley. Paper No.- SY177, In *Proc. International Workshop and Symposium on Industrial Drying (IWSID) – 2004*, UICT, Mumbai, India, December 20- 24, 2004.

Ingram, G. W. 1976. Deep bed drier simulation with intra-particle moisture diffusion. *Journal of Agricultural Engineering Research*, 21 (3): 263-272.

Jensen, C. A., Reed, R. D., Marks, R. J (II), M. A. El-Sharkawi, and J. Jung. 1999. Inversion of Feed forward Neural

- Networks: Algorithms and Applications. In *Proc. the IEEE*, 87(9): 1536-1549.
- Kindermann, J., and A. Linden. 1990. Inversion of neural networks by gradient descent. *Parallel Computing*, 14 (3): 277-286.
- Lu, B. L., H. Kita, and Y. Nishikawa. 1999. Inverting Feed Forward Neural Networks Using Linear and Nonlinear Programming. *IEEE Transactions on Neural Networks*, 10 (6): 1271-1290.
- Mandas, N., and M. Habte. 2002. Numerical simulation of static bed drying of barley. *Biosystems Engineering*, 82 (3): 313-319.
- O'Callaghan, J. R., D. J. Menzies, and P. H. Bailey. 1971. Digital simulation of agricultural drier performance. *Journal of Agricultural Engineering Research*, 16 (3): 223-244.
- Sharp, J R. 1982. A review of low temperature drying simulation models. *Journal of Agricultural Engineering Research*, 27 (3): 169-190.
- Sun, Da-Wen, and Woods, J. L. 1997. Simulation of the heat and moisture transfer process during drying in deep grain beds. *Drying Technology*, 15 (10): 2509-2525.